J Braz. Soc. Mech. Sci. Eng. (2017) 39:41–51
DOI 10.1007/s40430-015-0481-7

TECHNICAL PAPER

# Vertical dynamic analysis of a quarter car suspension system with MR damper

**K. Hemanth[1] · Hemantha Kumar[1] · K. V. Gangadharan[1]**

Received: 16 November 2015 / Accepted: 13 December 2015 / Published online: 21 January 2016
© The Brazilian Society of Mechanical Sciences and Engineering 2016

**Abstract** This paper presents ride comfort and road holding analysis of passive and semi-active suspension system using quarter car model. Semi-active suspension system with magnetorheological (MR) damper was modeled as non-parametric model-based magnetic flux density in the fluid flow gap. The skyhook control strategy was used to analyze semi-active control performance. The simulation of passive and semi-active suspension system was carried out under random road profile for different velocities. The result shows that semi-active suspension has significant improvement in terms of ride comfort and road holding of vehicle than passive suspension system. Experimental studies have been conducted to characterize MR damper and a good match is observed between results with simulation results obtained using non-parametric model.

**Keywords** MR damper · Non-parametric model · Skyhook control · Ride comfort and road holding

## 1 Introduction

In current scenario, improvements of driving safety and comfort are over lasting subjects in the vehicle design. It is not only a need, but also as a challenge for engineers to develop best quality of vehicle to attain superior performance. Ride comfort problems arise from vibrations of the vehicle, which may be due to a variety of sources like road surfaces irregularities, aerodynamic forces, vibrations of the engine and transmission. A strong demand for good suspension system exists to mitigate the vibrations that are being transmitted from road surface to the vehicle body.

Vehicle suspension system is responsible for isolating the vibrations of the vehicle body to achieve ride comfort and safety. A good ride comfort requires a soft suspension, whereas a hard suspension is required for carrying heavy loads. A good handling of vehicles requires a suspension system which makes better trade-off between two above-stated criteria [1]. To fulfill these conflicting requirements, a fully active or semi-active suspension system is preferred over a conventional passive suspension system. Active suspension system possesses inherent drawbacks as it necessitates large power requirement to drive external energy source. The cost of suspension system will be high and complex and difficulties arise while implementation of control hardware.

Semi-active suspension system combines the advantage of the active suspension in terms of improved vehicle performance and the robustness of the passive suspension, without requiring large power source [2]. In semi-active suspension, the amount of damping can be tuned in real time. The variation of damping may be achieved by varying the viscosity of the fluid under the influence of electric or magnetic field. Electrorheological (ER) and MR dampers are semi-active control devices that use ER and MR fluids to produce controllable damping force. MR fluids are similar to ER fluid, but MR fluids are 20–50 times stronger than ER fluid and it can be activated from low-voltage power supply (less than 10 V and 1–2 A). MR fluids are far less sensitive to contamination and extreme temperature (150 °C and higher). Butz and Von [3] presented an overview on properties of MR and ER fluid. Also, the various

Technical Editor: Kátia Lucchesi Cavalca Dedini.

✉ Hemantha Kumar
hemanta76@gmail.com

[1] Department of Mechanical Engineering, NIT Karnataka, Surathkal, Mangalore 575025, India

models which can be used to predict the behavior of MR and ER fluid device and their applications were discussed. Shivaram and Gangadharan [4] designed a statistical model of MR damper using the design of experiment approach; various factors such as magnetic field strength, volume fraction of the magnetic particle, shearing gap between piston and cylinder, amplitude and frequency of vibration were considered in their experimentation. Chooi et al. [5] described the general expression of yield stress and studied the effect of yield stress of fluid flow through the annuli by utilizing derived general expression. They also carried out that computational fluid dynamic analysis to validate with the obtained general expression. Costa and Branco [6] conducted experimental and analytical evaluation of MR damper and also studied the friction force effect between MR fluid and the device wall. Avinash et al. [7] developed the twin tube MR damper and conducted an experiment to analyze the damping characteristic of MR damper under different conditions such as air damping, viscous damping and MR damping. Boada et al. [8] conducted dynamic analysis of an MR damper under sinusoidal excitation. They used recursive lazy learning method to predict the response of MR damper. Metered et al. [9] carried out experimentation to study the dynamic characteristics of an MR damper and used feed forward recurrent neural network method to predict the behavior of MR damper. Ekkachai and Nilkhamhang [10] proposed a novel method to study the hysteresis behavior of MR damper using elementary hysteresis model (EHM) and feed forward neural network (FNN). Du et al. [11] and Nitin et al. [12] conducted an experiment on MR damper prototype under cyclic excitation and a polynomial function has been considered to predict MR damper behavior. Also they analyzed semi-active H-infinity control strategy for vehicle suspension with MR damper. Song et al. [13] studied the non-parametric modeling approach to predict the behavior of MR damper; they used series of continuous and differentiable mathematical functions to represent the characteristics of the physical damper. Hemanth et al. [14] considered the magnetic saturation analysis of magnetorheological damper for single coil and double coil arrangement using FEM (finite element method) and developed non-parametric model based on magnetic flux density in the fluid flow gap. Goldasz and Sapinski [15] conducted the magneto-static analysis of MR damper using FEM and numerical simulation with two different operation modes (flow and squeeze mode). Parlak et al. [16] designed of magnetorheological damper using FEM and also analyzed MR fluid behavior using computational fluid dynamic (CFD) analysis. Guan et al. [17] presented finite element analysis and multi-objective optimization (genetic algorithm) for MR damper. The fifth-order polynomial was considered to relate the shear stress and magnetic flux density. Rao et al. [18] evaluated the ride comfort of off-road vehicles by replacing the normal passive damper with controllable, two-state, semi-active damper and compared with passive suspension system. Alexandru and Alexandru [19] made comparative study between passive suspension and active suspension of motor vehicle by passing over bump dynamic regime. Abdolvahab et al. [20] studied the active quarter car suspension system with linear quadratic control (LQR) technique under different road condition and compared the results with passive quarter car suspension system. Chen [21] proposed skyhook surface sliding mode control method to semi-active vehicle suspension system for its ride comfort enhancement. Gopala and Narayanan [22] reported dynamic response using two degrees of freedom quarter car model with nonlinear passive elements traversing a rough road with skyhook control strategy. Yoshimura et al. [23] developed an active suspension system for a quarter car model using the concept of sliding mode control. Prabakar et al. [24] investigated control of the stationary response of a quarter car model to random road excitation with an MR damper as a semi-active suspension device. Sireteanu and Stoia [25] optimized the system nonlinear damping characteristics for passive and semi-active suspension with respect to ride comfort criterion. Kurczyk and Pawełczyk [26] studied semi-active control of suspension of an all-terrain vehicle using fuzzy control compared with Skyhook control. Guo and Zhang [27] identified the optimal placement of magnetorheological fluid damper for structural control using genetic algorithm.

Significant work has been carried out in the area of development of MR damper. This paper attempts a novel approach using non-parametric model based on magnetic flux density obtained in fluid flow gap. The proposed non-parametric model for MR damper has been validated with experimental investigations. Also ride comfort and road holding capabilities of a semi-active suspension system using quarter car model with skyhook control is analyzed.

## 2 Experimental analysis of MR damper

The MR damper consists of a piston having electromagnetic coil, inner cylinder and outer cylinder. The components of twin tube MR damper are as shown in Fig. 1. The designed dimension of twin tube MR damper is given in Table 1. The electromagnetic circuit in the piston consist of 1000 number of turns and subjected up to a maximum current of 1 A and 9 V electric potential. The MR valve arrangement of twin tube MR damper is as shown in Fig. 2. It is observed that the 1.5 mm gap is provided around the piston for fluid flow, instead of providing flow gap through piston core. In twin tube damper, when the piston moves the fluid displaces from inner cylinder to the outer reservoir and the amount of fluid displaced from inner cylinder

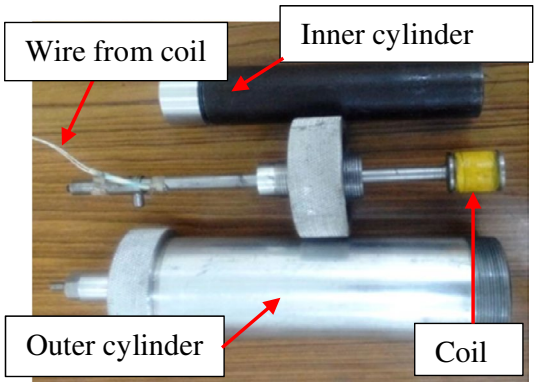


**Fig. 1** Component of MR damper

**Table 1** Dimension of twin tube MR damper

| Parameters | Dimensions (mm) |
|---|---|
| Inner diameter of inner cylinder | 28 |
| Thickness of inner cylinder ($t_1$) | 5 |
| Inner diameter of the outside cylinder | 46 |
| Thickness of outer cylinder ($t_2$) | 9 |
| Distance between poles ($l$) | 21 |
| Pole length ($L$) | 2 |
| Radial distance from piston rod to coil width ($h$) | 7.5 |
| Coil width ($w$) | 5 |
| Clearance between piston and inner cylinder ($g$) | 1.5 |

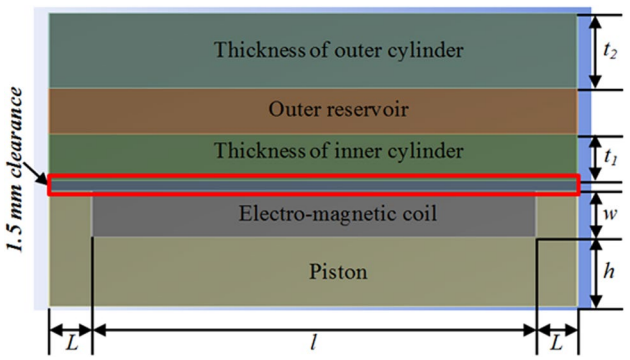


**Fig. 2** MR valve of twin tube MR damper

to outer reservoir is equal to the volume of fluid displaced by the piston rod as it enters into the inner housing.

To study the dynamic behavior of MR damper, experimentation was carried out using a custom-built damper testing machine as shown in Fig. 3. The main components of the damper testing machine are shaker, linear variable differential transformer (LVDT), force transducer and a data acquisition system. The APS 420 ELECTRO-SEIS electrodynamics shaker was used for exciting the MR damper. The

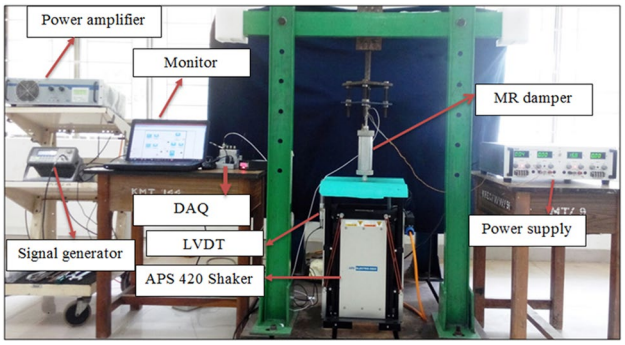


**Fig. 3** MR damper test setup

shaker has a rated sine peak force 900 N with frequency range of 1–200 Hz. The rated peak to peak amplitude/displacement is 150 mm. It can be operated manually or in PC-based control mode and compatible to PC-based data actuation. APS 145 power amplifier was used in the voltage mode to produce constant velocity.

In present study, 30 percent volume fraction of carbonyl iron particles with diameter of 6.23 μm was dispersed in silicon oil. To reduce the sedimentation of particle, grease was added as stabilizer. The damper test was performed at 1.5 and 2 Hz frequencies for different current values. Current varied from 0.1–0.4 A (increment of 0.1 A) with a sinusoidal signal of ±0.005 m amplitude. The current is monitored and supplied through DC power supply (0–64 V/5 A Max.). The damping force experienced by the piston rod was sensed by a force transducer fitted at the top of the piston rod and the displacement was measured through LVDT. The dynamic characteristic of MR damper is analyzed using the force v/s velocity and force v/s displacement curves as discussed in Sect. 6.

## 3 Magneto-static analysis

The study of the MR damper is a promising topic as it provides controllable damping force by varying the current in the electromagnetic coil. In the MR damper, the damping force developed is highly influenced by magnetic flux density in the fluid flow gap. For this reason magneto-static analysis of MR damper is very crucial to understand the variation of magnetic flux density in the fluid flow gap. Hence, the finite element model of twin tube MR damper has been built (as per the designed dimension in Table 1) and analyzed using ANSYS. The finite element model of twin tube MR damper is as shown in the Fig. 4. Because of symmetrical geometry only one-fourth of computational domain has been constructed for the analysis. In this FEM analysis, the piston and inner cylinder are taken as steel and the outer cylinder

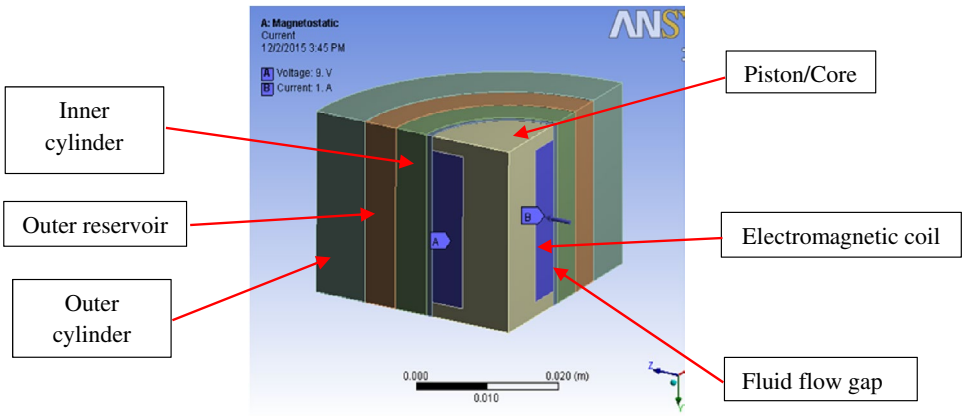


**Fig. 4** Finite element modeling of MR damper

**Table 2** Magnetic properties of MR damper component

| Material | Relative permeability |
|---|---|
| Steel (SA1008) | B–H curve (Fig. 5) |
| Copper | 1 |
| MR fluid (MRF132-DG) | B–H curve (Fig. 6) |
| Aluminum alloy | 1 |

is considered as aluminum alloy. The properties of MR damper component are given in the Table 2. The electromagnetic circuit in the piston consists of 1000 number of turns and it is subjected to a maximum current of 1 A and 9 V electric potential and the boundary condition is mentioned in Fig. 4. In this analysis certain assumptions are considered, which are as follows

- There is no leakage of flux from the body of cylinder.
- The magnetic flux lines are parallel along the symmetric plane.

Figures 5 and 6 depict the typical magnetic properties of the steel (SA1008) and MR fluid (LORD MRF132-DG) and it signifies the saturation of the material. In saturable materials the permeability is not constant; it depends on magnetic field strength. The magnetic flux density increases proportionally to magnetic field strength up to certain limit; there after the magnetic flux density is not increased further, even though the magnetic field strength continues to increase.

The static magnetic analysis of MR damper provides the nodal solution at the clearance space (fluid flow gap) of MR damper under its magnetic induction. The total magnetic flux density of MR damper at fluid flow gap is as shown in Fig. 7.

The entire fluid flow gap is divided into five categories based on the maximum and minimum total magnetic flux density for corresponding current value. In this classification

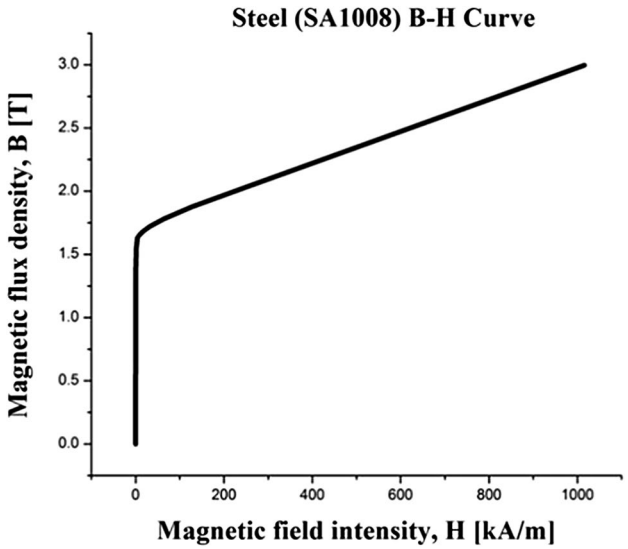


**Fig. 5** B–H curve of steel

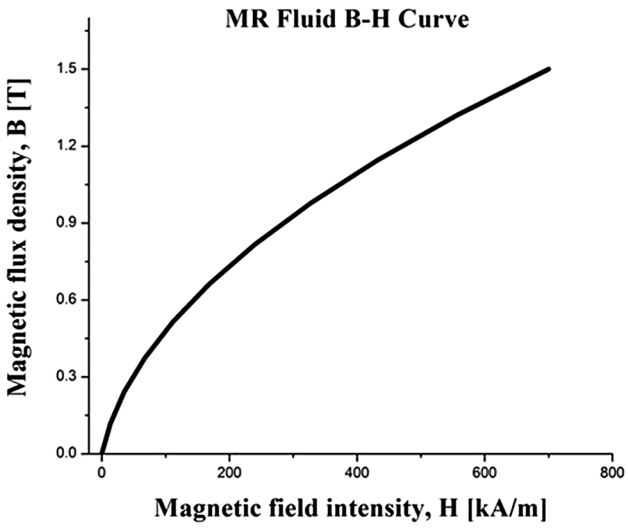


**Fig. 6** B–H curve of MR fluid

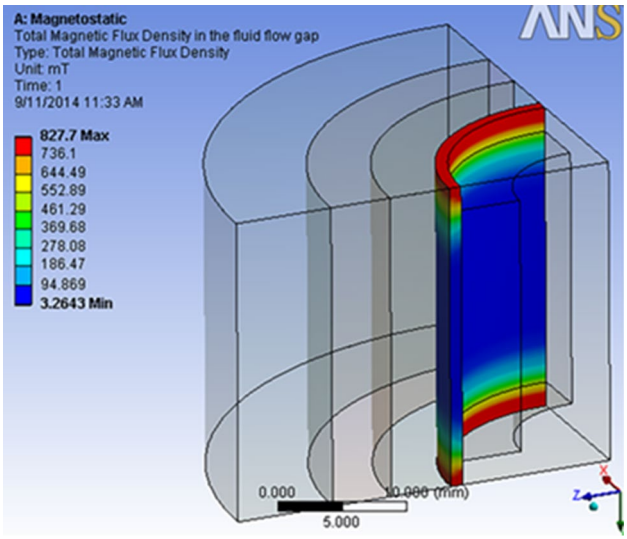


**Fig. 7** Total magnetic flux density in the fluid flow gap

method, each class consists of an equal data interval. The step length is calculated using following formula,

$$\text{Step length} = \frac{\text{Range of data}}{\text{Number of categories required}} = \frac{\text{Max. total magnetic flux density} - \text{Min. total magnetic flux density}}{\text{Number of categories required}}$$

The categorized data are given in the Table 3. The summation of average total magnetic flux density values are used to relate the force and applied current.

### 3.1 Non-parametric model for MR damper

Non-parametric approach employs analytical expression to describe the characteristics of modeled device and it is highly useful for studying the linear, nonlinear behavior of a system. The advantage of the non-parametric modeling methods is that they can avoid the pitfalls of parametric approaches while being robust and applicable to linear, nonlinear and hysteresis system [28]. This paper presents novel approach to study the non-parametric model characterization of an MR damper.

The magnetic flux density obtained from the magnetostatic analysis of MR damper for different values of current is categorized using the statistical data categorizing technique. The damping force is calculated for each current value using Eq. (1).

Force due to applied magnetic field is

$$F_d = \frac{A\sum(B_i \times n_i)}{2\pi\mu_0\mu_r},\ i = 1, 2, 3 \tag{1}$$

where

$F_d$ is the force in Newton.

$B_i$ is the magnetic field in Tesla.

$n_i$ is the number of suspended particles in the categorized region of the fluid flow gap.

$A$ is the surface area of the suspended particles in $m^2$.

$\mu_0$ is the permeability of the free space ($4\pi \times 10^{-7}$ H/m).

$\mu_r$ is the relative permeability of MR fluid.

Polynomial model is one of the most commonly used non-parametric models. It is used to describe the force is a function of the current ($I$) applied to the MR damper. The hysteresis loop of MR damper is fitted by polynomial with sinusoidal displacement function [$x = a \sin(2\pi ft)$].

$$F_d = \sum_{i=0}^{n} \left(\alpha_i I^i\right) x \tag{2}$$

where $n$ is the order of polynomial, and fifth-order polynomial function is considered to establish relation between the damping force and applied current.

$$F_d = (\alpha_1 I^5 + \alpha_2 I^4 + \alpha_3 I^3 + \alpha_4 I^2 + \alpha_5 I + \alpha_6)x \tag{3}$$

where $I$ is the applied current in 'A' and coefficient of the equation are constants determined by curve fitting ($\alpha_1 = -7782$, $\alpha_2 = 2.126\text{e}+04$, $\alpha_3 = -2\text{e}+04$, $\alpha_4 = 6578$, $\alpha_5 = 849$, $\alpha_{5=-29.49}$).

## 4 Mathematical modeling of quarter car model

A quarter car model with two degrees of freedom system is analyzed by considering vertical movement of the suspension system as shown in Fig. 8. The quarter car model consists of sprung mass ($M_s$), unsprung mass ($M_u$) and MR damper, which is modeled as non-parametric model. The damping coefficient of the tire is represented as $C_t$ and $F_d$ is the variable damping force developed by the MR damper. $K_s$ and $K_t$ are the stiffness of the suspension system and tire, respectively. $x_s$ and $x_u$ represent the displacement of sprung and unsprung mass. $W$ is the road displacement. The equation of motion of a quarter car suspension system can be derived by applying Newton's second law of motion.

$$\begin{aligned} &M_s\ddot{x}_s + K_s(x_s - x_u) + F_d = 0 \\ &M_u\ddot{x}_u + C_t(\dot{x}_u - \dot{W}) + K_s(x_u - x_s) \\ &\quad + K_t(x_u - W) - F_d = 0 \end{aligned} \tag{4}$$

**Table 3** Categorized data

| Current (A) | Average total magnetic flux density (mT) | Percentage of exposure | Average total magnetic flux density (mT) | Percentage of exposure | Average total magnetic flux density (mT) | Percentage of exposure | Average total magnetic flux density (mT) | Percentage of exposure | Average total magnetic flux density (mT) | Percentage of exposure |
|---|---|---|---|---|---|---|---|---|---|---|
| 0.1 | 8.76 | 59.44 | 96.93 | 4.63 | 157.34 | 6.45 | 221.30 | 3.69 | 285.24 | 25.79 |
| 0.2 | 17.15 | 59.44 | 163.77 | 4.63 | 244.03 | 4.63 | 334.18 | 5.51 | 450.67 | 25.79 |
| 0.3 | 25.20 | 59.44 | 180.33 | 1.87 | 292.459 | 7.38 | 433.00 | 5.51 | 576.82 | 25.79 |
| 0.4 | 31.11 | 59.44 | 207.72 | 1.87 | 332.35 | 7.38 | 487.35 | 5.51 | 645.03 | 25.79 |
| 0.5 | 35.54 | 59.44 | 223.21 | 1.87 | 353.92 | 7.38 | 516.04 | 5.51 | 680.58 | 25.79 |
| 0.6 | 36.22 | 57.62 | 194.80 | 3.69 | 372.63 | 7.38 | 540.68 | 5.51 | 710.91 | 25.79 |
| 0.7 | 40.15 | 57.62 | 206.10 | 3.69 | 389.71 | 7.38 | 561.88 | 5.41 | 737.80 | 25.89 |
| 0.8 | 43.98 | 57.62 | 216.54 | 3.69 | 404.66 | 7.33 | 569.36 | 4.63 | 758.53 | 26.73 |
| 0.9 | 47.73 | 57.62 | 226.26 | 3.69 | 407.81 | 6.45 | 572.90 | 5.51 | 780.43 | 26.73 |
| 1 | 49.41 | 56.68 | 2288.74 | 4.63 | 420.69 | 6.45 | 588.97 | 5.51 | 800.49 | 26.73 |

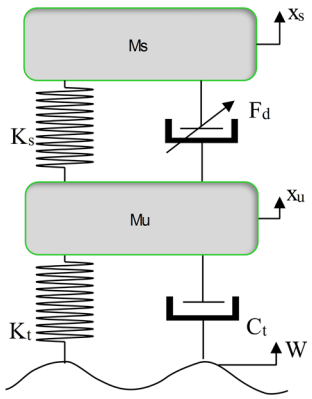


**Fig. 8** Quarter car model with semi-active suspension

**Table 4** Parameters of quarter car suspension system

| Parameters | Value |
|---|---|
| Sprung mass ($M_s$) | 214.5 kg |
| Unsprung mass ($M_u$) | 41.5 kg |
| Stiffness of spring ($K_s$) | 6000 N/m |
| Tire stiffness ($K_t$) | 140,000 N/m |
| Suspension damping coefficient ($C_s$) | 300 Ns/m |
| Tire damping coefficient ($C_t$) | 1500 Ns/m |

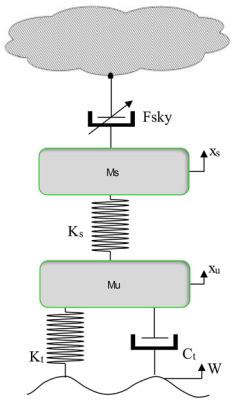


**Fig. 9** Skyhook control strategy

The above equation can be written in the form of state space variables given by

$$\left.\begin{aligned}\dot{x} &= Ax + Bu\\ y &= Cx + Du\end{aligned}\right\} \tag{5}$$

where

$$x = \begin{bmatrix} x_s & x_u & \dot{x}_s & \dot{x}_u \end{bmatrix}^T \quad u = \begin{bmatrix} F_d & W & \dot{W} \end{bmatrix}^T$$

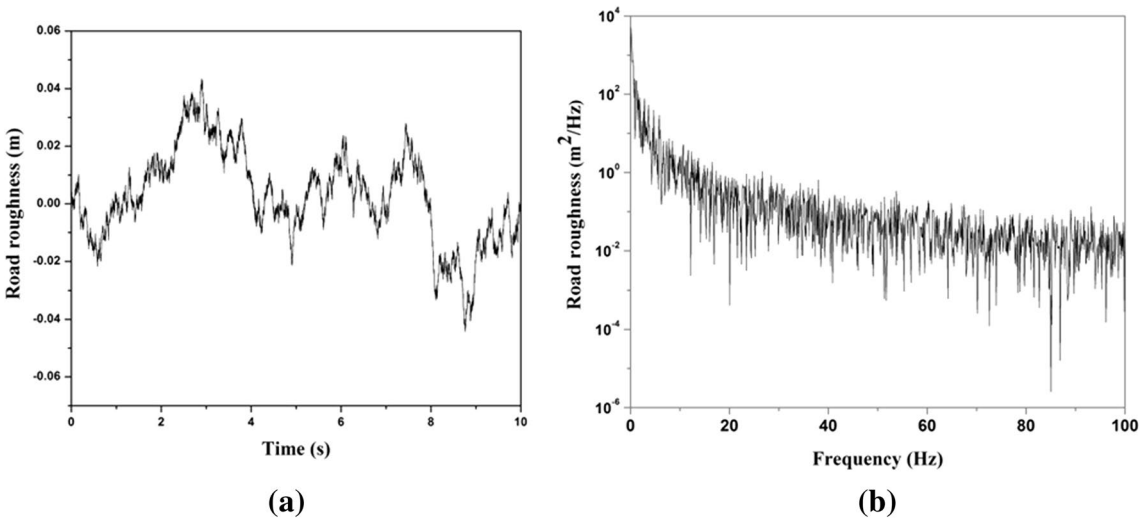


**Fig. 10** **a** Random road roughness profile in time domain and **b** PSD of random road roughness profile

**Table 5** Road roughness value for different classes of road

| Degree of road roughness $G_q(\Omega_0)$ [$10^{-6}$m$^2$/(cycle/min)] at $n_0 = 0.1$ cycle/min | |
|---|---|
| Road classes | Geometric mean |
| A (very good road) | 16 |
| B (good road) | 64 |
| C (average road) | 256 |
| D (poor road) | 1024 |
| E (very poor road) | 4096 |

$$A = \begin{bmatrix} 0 & 0 & 1 & 0 \\ 0 & 0 & 0 & 1 \\ -\frac{K_s}{M_s} & \frac{K_s}{M_s} & 0 & 0 \\ \frac{K_s}{M_u} & -\left(\frac{K_s+K_t}{M_u}\right) & 0 & \frac{-C_t}{M_u} \end{bmatrix} \quad B = \begin{bmatrix} 0 & 0 & 0 \\ 0 & 0 & 0 \\ -\frac{1}{M_s} & 0 & 0 \\ \frac{1}{M_u} & \frac{K_t}{M_u} & \frac{C_t}{M_u} \end{bmatrix}$$

$$C = \begin{bmatrix} 1 & -1 & 0 & 0 \end{bmatrix} \quad D = \begin{bmatrix} 0 & 0 & 0 \end{bmatrix}$$

Parameters of quarter car suspension system are given in Table 4 [29].

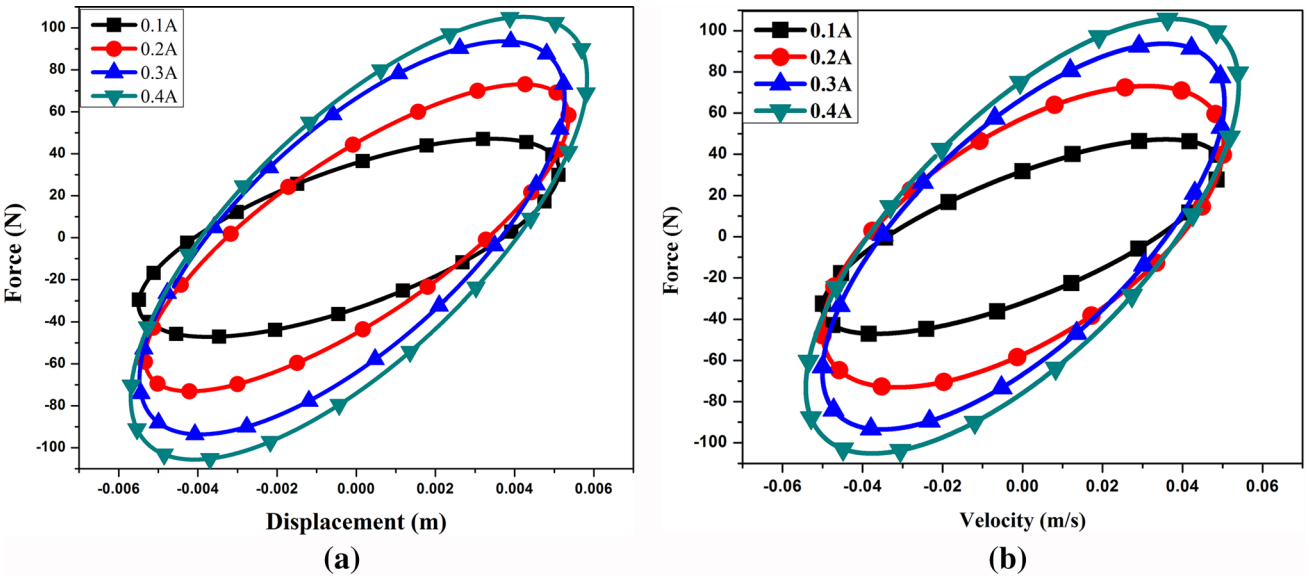


**Fig. 11** **a** Force v/s displacement and **b** Force v/s velocity of experimental result for 1.5 Hz

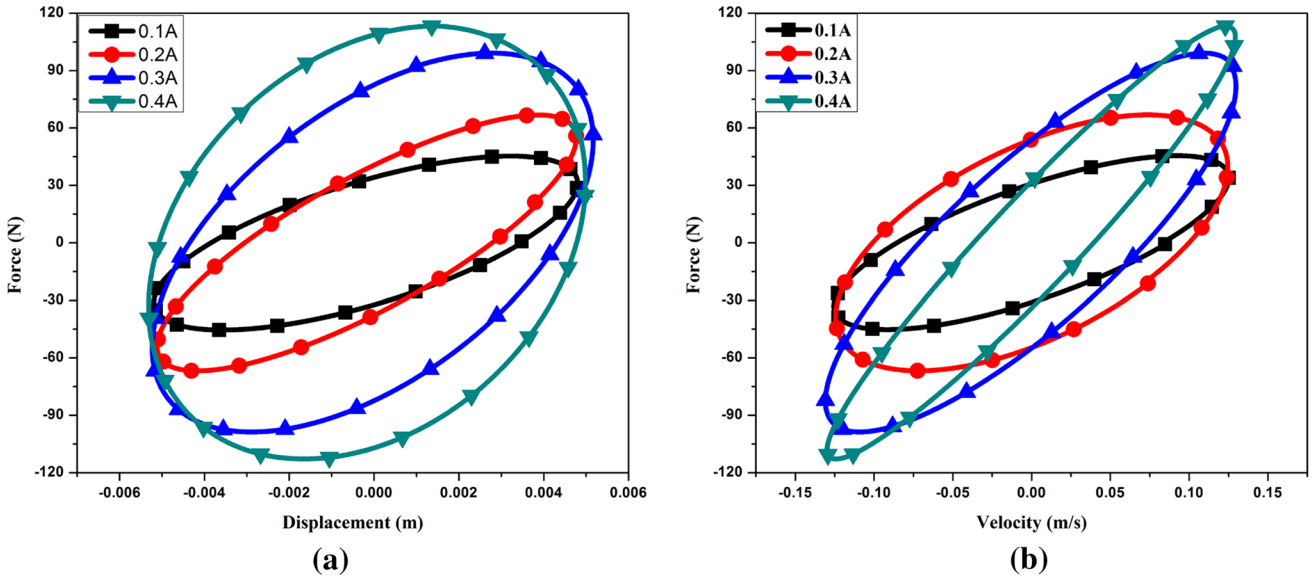


**Fig. 12** **a** Force v/s displacement and **b** force v/s velocity of experimental result for 2 Hz

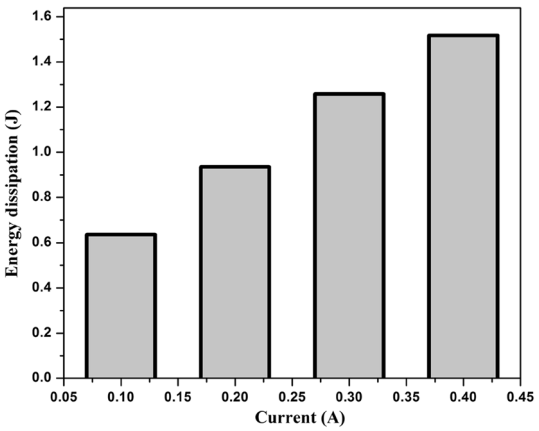


**Fig. 13** Current v/s energy dissipation

### 4.1 Semi-active control strategy

Skyhook controller is a popular and an effective vibration control method, because it can dissipate system energy at a higher rate. The skyhook control can reduce the resonant peak of the sprung mass quite significantly and provide good handling performance of the vehicle. As the name itself indicates the damper is connected to the some inertial reference in the sky. The skyhook control strategy is as shown in Fig. 9.

The main aim of the skyhook controller is to reduce the RMS acceleration of the sprung mass. The skyhook control strategy is given in Eq. (6).

$$F_{\text{sky - hook}} = \begin{cases} F_{\max}, & if\, \dot{x}_s(\dot{x}_s - \dot{x}_u) > 0 \\ F_{\min}, & if\, \dot{x}_s(\dot{x}_s - \dot{x}_u) \leq 0 \end{cases} \quad (6)$$

The skyhook strategy indicates that if the relative velocity between body and wheel is in the same direction as that of body velocity, then maximum damping force should be applied to reduce the body acceleration. If these two velocities are in the opposite direction, then minimum damping force should be applied.

## 5 Random road profile

When vehicle travels at constant velocity, the road roughness is viewed as stationary process in space domain. The PSD (power spectral density) random road distribution can be expressed as [30].

$$\dot{Z}_r(t) = -2\pi u n_0 Z_r(t) + \sqrt{G_q(\Omega_0) u w(t)} \quad (7)$$

where $Z_r(t)$ is road roughness amplitude, $G_q(\Omega_0)$ is random road roughness coefficient and it is constant for different grades of road, u is the vehicle forwarded velocity, $w(t)$ is the white noise signal, whose power spectral density is unity and $\omega_o$ is the lowest cutoff angular frequency given by

$$\omega_o = 2\pi f_0 \quad (8)$$

When vehicle moving at constant velocity u, the relation between frequency and vehicle forwarded velocity is given by

$$f_0 = u n_0 \quad (9)$$

where $n_0$ is reference spatial frequency ($n_0$), the value of $n_0 = 0.1$ cycle/min.

Equation (7) becomes,

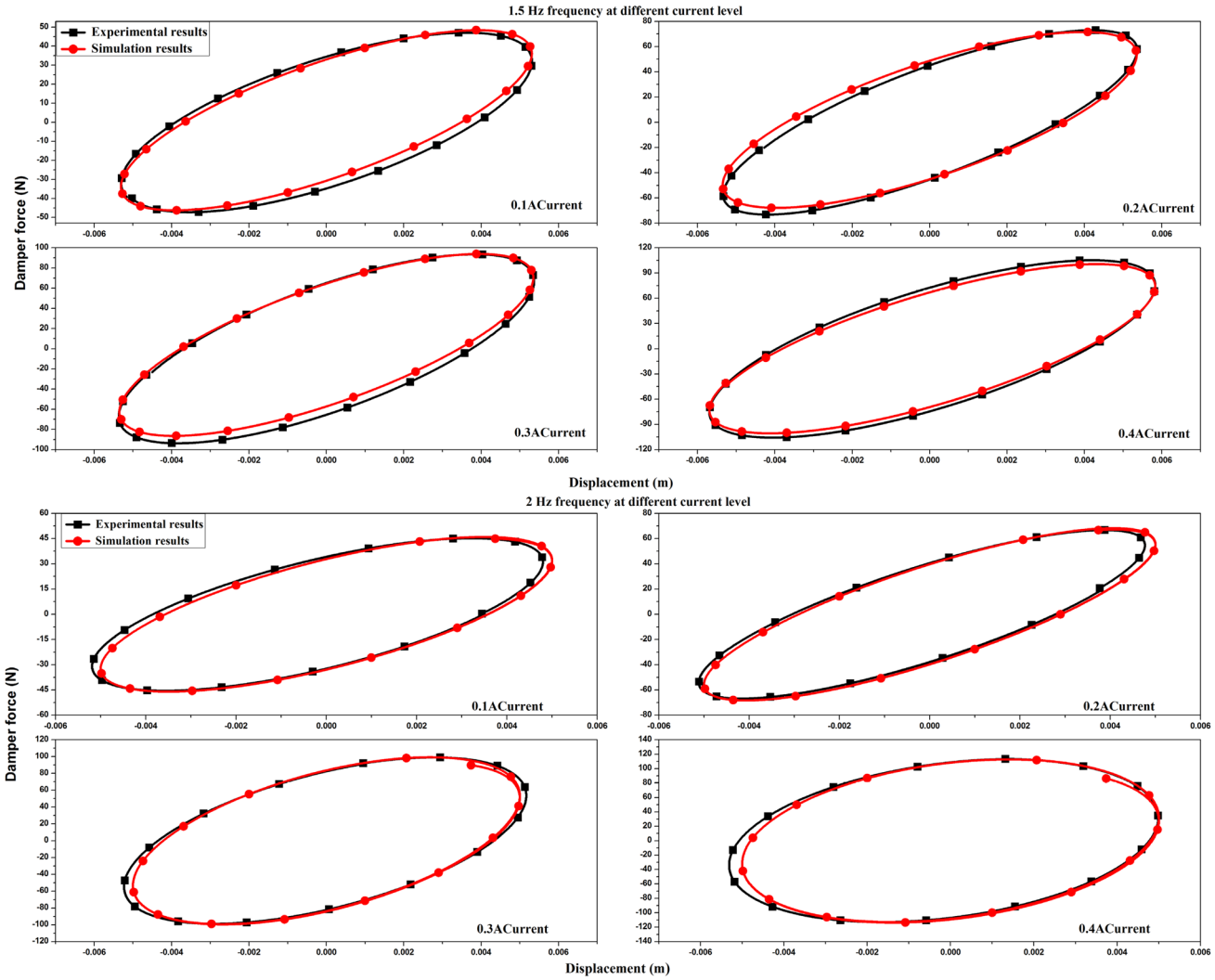


**Fig. 14** Force comparison between experimental and simulation data at different frequencies

$$\dot{Z}_r(t) = -2\pi u n_0 Z_r(t) + \sqrt{G_q(\Omega_o) u w(t)} \tag{10}$$

Figure 10a, b shows the random road roughness profile in time domain and its PSD, when vehicle move at 25 m/s on C-level road. Based on the pavement roughness, International Organization for Standardization (ISO-8606) classified the road into eight classes, indicated by letters A–H. Those from A–D classes are for hard surface road and its roughness values are given in Table 5 [31, 32]. In this classification we have chosen average road (C-level road) to evaluate the performance of quarter car suspension system.

## 6 Result and discussion

The fabricated MR damper was tested at 1.5 and 2 Hz frequencies for different current values under sinusoidal excitation. The dynamic behavior of an MR damper was analyzed using force v/s displacement and force v/s velocity curve as shown in Figs. 11 and 12. From observation, at lower input current the damping force is less and it increases gradually with increase in current. In addition, the slope of the curve increases with increase in current, which indicates increase in stiffness.

The energy dissipation of MR damper can be found from the area enclosed under the force v/s displacement curve for a particular current input, excitation frequency and amplitude. Figure 13 depicts energy dissipation with current and it can be noted that energy dissipation increases with increase in current.

Figure 14 illustrates damping force comparison between experimental and simulation results at different frequencies and different current levels, a good agreement is observed between them.

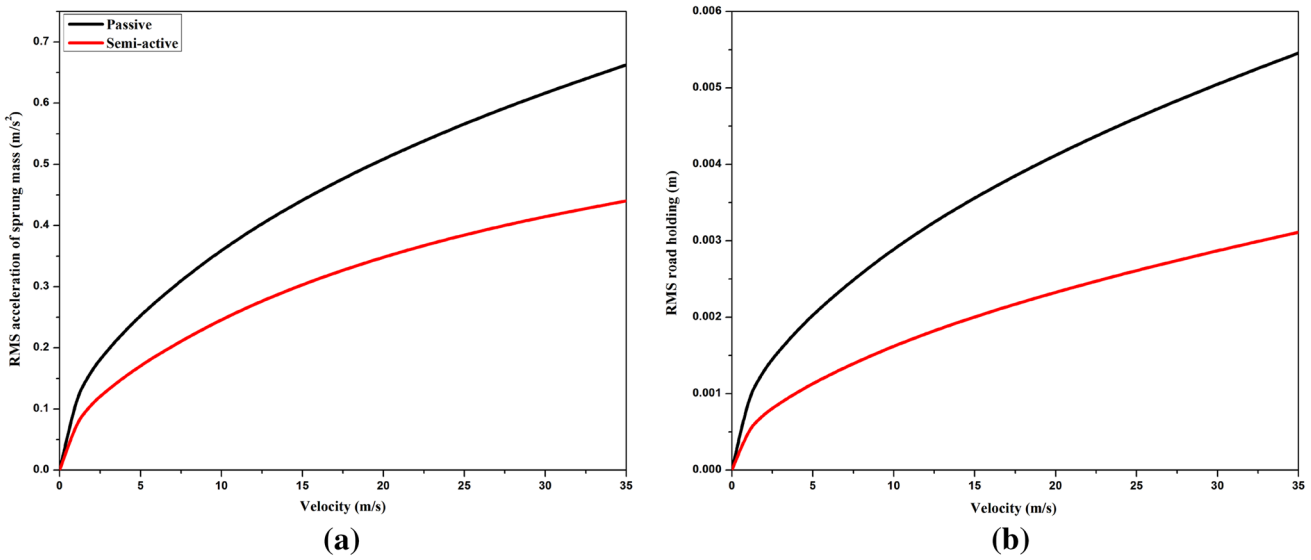


**Fig. 15** **a** RMS acceleration v/s velocity **b** RMS road holding v/s velocity

The simulation of two degrees of freedom quarter car model was carried out with passive and semi-active (MR damper) suspension. The developed non-parametric model was used as MR damper in semi-active suspension system. The quarter car modeling of both passive and semi-active suspension systems were simulated under random road roughness for different velocities. The RMS of the sprung mass acceleration response of both passive and semi-active suspension for different velocities is as shown in Fig. 15a. In semi-active suspension system it can be observed that the increase in velocity results in significant decrement in vertical acceleration of sprung mass. This indicates better ride comfort for a vehicle with semi-active suspension system.

Figure 15b illustrates the road holding response, which measures the relative displacement between the unsprung mass and road displacement with respect to different velocities. In this case also road holding will be better with semi-active suspension than passive suspension for all velocities.

## 7 Conclusion

This paper discussed about characterization of MR damper at 1.5 Hz frequency for different current values. Current is varied from 0.1 A to 0.4 A with (increment of 0.1 A) sinusoidal excitation. Result demonstrates that damping force increases with increase in current, which leads to increase in energy dissipation and stiffness. Also a novel method of non-parametric model for MR damper has been proposed. The non-parametric model was developed and analyzed based on magnetic flux density in the fluid flow gap and volume fraction of MR fluid. A good agreement has been observed between simulation results and experimental results.

A two degrees of freedom quarter car suspension with MR damper was modeled as non-parametric model. The vehicle model was simulated under random road roughness for different velocities. The result shows that good ride comfort and road holding of vehicle for different velocities provide significant improvement in semi-active suspension with MR damper than passive suspension system.

**Acknowledgments** The authors acknowledge the funding support from Department of Science and Technology (DST): No.SB/FTP/ETA-0071/2013 and also acknowledge SOLVE Lab: The Virtual Lab @ NITK (http://www.solve.nitk.ac.in) and Centre for System Design (CSD): A Centre of excellence at NITK-Surathkal for providing experimental facility.

## References

1. Liu Y, Waters TP, Brennan MJ (2005) ) A comparison of semi-active damping control strategies for vibration isolation of harmonic disturbances. J Sound Vib 280(1):21–39
2. Harris CM (1987) Shock and vibration handbook. McGraw-Hill, New York
3. Butz T, Von Stryk O (2002) Modelling and simulation of electro- and magnetorheological fluid dampers. ZAMM 82(1):3
4. Shivaram AC, Gangadharan KV (2007) Statistical modelling of a magneto-rheological fluid damper using the design of experiments approach. Smart Mater Struct 16(4):1310
5. Chooi WW, Oyadiji SO (2008) Design, modelling and testing of magnetorheological (MR) dampers using analytical flow solutions. Comput Struct 86(3):473–482
6. Costa E, Branco PJ (2009) Continuum electro mechanics of a magnetorheological damper including the friction force effects

between the MR fluid and device walls Analytical modelling and experimental validation. Sens Actuators 155(1):82–88
7. Avinash B, Sundar SS, Gangadharan KV (2014) Experimental study of damping characteristics of air, silicon oil, magneto rheological fluid on twin tube damper. Int Conf Adv Manuf Mater Eng NITK 5:2258–2262
8. Boada MJL, Calvo JA, Boada BL, Diaz V (2011) Modeling of a magnetorheological damper by recursive lazy learning. Int J Non-Linear Mech 46(3):479–485
9. Metered H, Bonello P, Oyadiji SO (2010) The experimental identification of magnetorheological dampers and evaluation of their controllers. Mech Syst Signal Process 24(4):976–994
10. Ekkachai K, Nilkhamhang I (2012) MR damper identification using EHM-based feed forward neural network. In SICE Annual Conference Proceedings of IEEE, Akita University, 1138–1143
11. Du H, Yim Sze K, Lam J (2005) Semi-active H∞ control of vehicle suspension with magneto-rheological dampers. J Sound Vib 283(3):981–996
12. Ambhore NH, Pangavhane DR, Hivarale SD (2013) A study of some nonparametric model of magnetorheological fluid damper for vibration control. Int J Curr Eng Technol 3:388–392
13. Xubin Song, Ahmadian Mehdi, Southward Steve C (2005) Modelling MR dampers with application of nonparametric approach. J Intell Mater Syst Struct 16(5):421–432
14. Hemanth K, Ganesha A, Kumar Hemantha, Gangadharan KV (2014) Analysis of MR damper based on finite element approach. Appl Mech Mater 592:2006–2010
15. Gołdasz J, Sapinski B (2011) Modelling of magnetorheological mounts in various operation modes. acta mechanica et automatica, *5*, 29–40
16. Parlak Z, Engin T, Call I (2012) Optimal design of MR damper via finite element analyses of fluid dynamic and magnetic field. Mechatronics 22(6):890–903
17. Guan X, Guo P, Ou J (2009) Multi-objective optimization of magnetorheological fluid dampers. Eng Mech 26:30–35
18. Rao M, Ram T, Purushottam A (2010) Analysis of passive and semi active controlled suspension systems for ride comfort in an omnibus passing over a speed bump. Int J Res Rev Appl Sci 5(1):7–17
19. Alexandru C, Alexandru P (2011) A comparative analysis between the vehicles passive and active suspensions. Int J Mech 5(4):371–378
20. Abdolvahab A, Chavan US, Phvithran DS (2012) Simulation and analysis of passive and active suspension system using quarter car model for non uniform road profile. Int J Eng Res Appl 2(5):900–906
21. Chen Y (2009) Skyhook surface sliding mode control on semi-active vehicle suspension system for ride comfort enhancement. Engineering 1(01):23
22. Gopala Rao LVV, Narayanan S (2009) Sky-hook control of non-linear quarter car model traversing rough road matching performance of LQR control. J Sound Vib 323:515–529
23. Yoshimura T, Kume A, Kurimoto M, Hino J (2001) Construction of an active suspension system of a quarter car model using the concept of sliding mode control. J Sound Vib 239(2):187–199
24. Prabakar RS, Sujatha C, Narayanan S (2013) Response of a quarter car model with optimal magnetorheological damper parameters. J Sound Vib 332(9):2191–2206
25. Sireteanu T, Stoia N (2003) Damping optimization of passive and semi-active vehicle suspension by numerical simulation. Proc Romanian Acad 4(2):121–127
26. Kurczyk S, Pawełczyk M (2013) Fuzzy control for semi-active vehicle suspension. Low frequency noise. Vibration and Active Control 32(3):217–226
27. Guo Zhang (2004) Optimal placement of MR dampers for structural control using identification crossover genetic algorithm. Low Freq Noise Vibration Active Control 23(3):167–178
28. Gangrou Peng (2011) Development of MR damper for motorcycle steering. ME thesis, University of Wollongong
29. Patil K S, Jagtap V, Jadhav S, Bhosale A, Kedar B (2013) performance evaluation of active suspension for passenger cars using MATLAB. In Second National Conference on Recent Developments in Mechanical Engineering. IOSR J Mech Civil Eng 06–14
30. He L, Qin G, Zhang Y, Chen L (2008) Non-stationary random vibration analysis of vehicle with fractional damping. Int Conf Intell Comput Technol Auto 2:150–157
31. Tyan F, Hong YF, Tu SH, Jeng WS (2009) Generation of random road profiles. J Adv Eng 4(2):1373–1378
32. Barbosa RS (2011) Vehicle dynamic response due to pavement roughness. Journal Brazilian Soc Mech Sci Eng 33(3):302–307